small NANO MICRO

Cellular Uptake and Cytotoxicity of Gold Nanorods: Molecular Origin of Cytotoxicity and Surface Effects

Alaaldin M. Alkilany, Pratik K. Nagaria, Cole R. Hexel, Timothy J. Shaw, Catherine J. Murphy, and Michael D. Wyatt**

Gold nanorods of different aspect ratios are prepared using the growth-directing surfactant, cetyltrimethylammonium bromide (CTAB), which forms a bilayer on the gold nanorod surface. Toxicological assays of CTAB-capped nanorod solutions with human colon carcinoma cells (HT-29) reveal that the apparent cytotoxicity is caused by free CTAB in solution. Overcoating the nanorods with polymers substantially reduces cytotoxicity. The number of nanorods taken up per cell, for the different surface coatings, is quantitated by inductively coupled plasma mass spectrometry on washed cells; the number of nanorods per cell varies from 50 to 2300, depending on the surface chemistry. Serum proteins from the biological media, most likely bovine serum albumin, adsorb to gold nanorods, leading to all nanorod samples bearing the same effective charge, regardless of the initial nanorod surface charge. The results suggest that physiochemical surface properties of nanomaterials change substantially after coming into contact with biological media. Such changes should be taken into consideration when examining the biological properties or environmental impact of nanoparticles.

Keywords:
- cellular uptake
- cytotoxicity
- gold nanorods
- surfaces

1. Introduction

Gold nanomaterials have unique optical properties that make them highly attractive candidates for biomedical applications such as drug and gene delivery,[1,2] biological imaging,[3–5] and cancer treatment.[6,7] However, unintended biological or environmental consequences of nanomaterial exposure is an emerging issue.[8] Systematic studies attempting to delineate the influence of physiochemical properties such as size, shape, effective surface charge, surface chemistry, and aggregation state of nanomaterials on their biological properties such as cellular uptake and cytotoxicity are appearing in the literature.[9–11] There are reports that interpret cytotoxicity data in terms of the original physiochemical properties of the nanomaterials, for example net charge.[11–16] However, cell-culture media contains electrolytes that can aggregate nanomaterials and serum proteins that can adsorb to nanomaterial surfaces, rapidly changing the surface charge/chemistry and the original nanomaterial dimensions.[17–19]

Here, we report that gold nanorods with well-defined dimensions and known initial surface chemistries[20,21] show more cytotoxicity than gold nanospheres at the same particle/cell concentrations in a human cancer cell line and that molecular desorption or residual contamination of starting materials, rather than the nanorods themselves, is the major cause of cytotoxicity. Importantly, we also show that the surface charge of the nanomaterials changes rapidly in media, likely due to the adsorption of serum proteins to the nanorod

[*] Prof. M. D. Wyatt, P. K. Nagaria
Department of Pharmaceutical and Biomedical Sciences
University of South Carolina
Columbia, SC 29208 (USA)
E-mail: wyatt@sccp.sc.edu
Prof. C. J. Murphy, Prof. T. J. Shaw, C. R. Hexel, A. M. Alkilany
Department of Chemistry and Biochemistry
University of South Carolina
Columbia, SC 29208 (USA)
E-mail: murphy@chem.sc.edu

Supporting Information is available on the WWW under http://www.small-journal.com or from the author.

DOI: 10.1002/smll.200801546

surfaces; we therefore believe that one possible mechanism of nanoparticles uptake is receptor-mediated endocytosis arising from cellular recognition of proteins from the media that have adsorbed onto the nanorods.

2. Results

We prepared a library of gold nanorods with different aspect (length/width) ratios and surface charges. These materials are popular for biomedical detection, imaging, and therapy.[1–7] Gold nanorod solutions were prepared using our wet-chemical methods that use the cationic surfactant cetyltrimethylammonium bromide (CTAB) as a structure-directing agent.[20] CTAB forms a chemisorbed bilayer on the surface of gold nanorods to display the cationic trimethylammonium head groups to the aqueous media.[22] Transmission electron microscopy (TEM) images of the gold nanorod library show excellent shape and size uniformity (Figure 1a). Layer-by-layer coating of purified CTAB-capped gold nanorods with net negatively charged (at neutral pH) polyacrylic acid (PAA) was used to flip the effective surface charge from positive to negative (Table S1 of Supporting Information).[21] Optical spectra of gold nanorods before and after coating were compared; the absence of broadening and tailing of the longitudinal plasmon peak indicates no nanoparticle aggregation (Figure 1b and c). Using the reported extinction coefficients of the longitudinal plasmon peaks,[23] all uncoated and coated gold nanorod solutions were normalized to the same molar concentration in nanoparticles (not gold atoms) for cellular assays.

Figure 2a shows cell viability of a human colon cancer cell line, HT-29 (10^3 cells), measured by the MTT assay,[24] after four days exposure to a concentration of 0.4 nM of CTAB-capped and PAA-coated gold nanorods of different aspect ratios. We found that all CTAB-capped gold nanorod solutions displayed a significant cytotoxicity at this concentration (65–75% loss of viability), independent of the aspect ratio. However, for all preparations, PAA overcoating almost eliminates the observed cytotoxicity at the same nanorod concentrations (Figure 2a). Cell growth was also determined by direct cell counting and the results confirmed that CTAB-capped gold nanorod solutions were growth inhibitory, while polymer-coated nanorods were not (Figure 2b).

The reduction in cytotoxicity associated with PAA overcoating led us to analyze the source of cytotoxicity associated with the CTAB-capped gold nanorod solutions. For the range of aspect ratios studied, the amount of bound CTAB corresponds to 1.2–5.5 μM. Free CTAB molecules are cytotoxic, reducing cell viability to 50% after 200 nM exposure for four days (Figure S1, Supporting Information), which suggests that polymer overcoating reduces the exposure of cells to CTAB. However, in this case, the polymer overcoating also flipped the effective surface charge. Previous studies[11–16] have implicated nanoparticle surface charge in cytotoxicity. In order to directly test charge effects, we overcoated the PAA-coated gold nanorods with the positively charged polyelectrolyte poly(allylamine) hydrochloride (PAH). A surface-terminated PAH coating converts the surface charge back to positive for the gold nanorods.[21] Figure 3a shows the viability of 10^3 HT-29 cells exposed to the same concentration (0.4 nM) of CTAB, PAA and PAH-coated gold nanorods for a

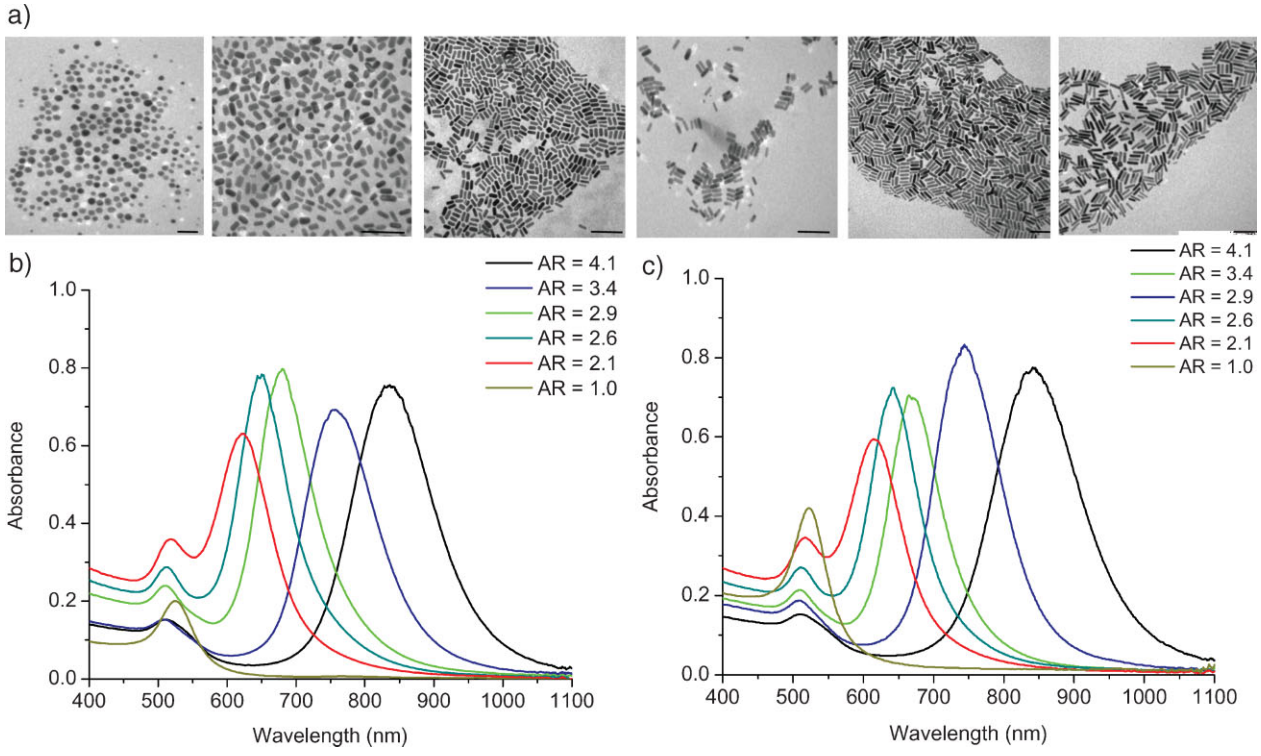

Figure 1. Physical characterization of the nanorods. a) TEM images of gold nanorods of different aspect ratios (AR). All scale bars = 100 nm. b) UV/Vis spectra of CTAB-capped gold nanorods. c) UV/Vis spectra of PAA-coated gold nanorods.

NANO MICRO small

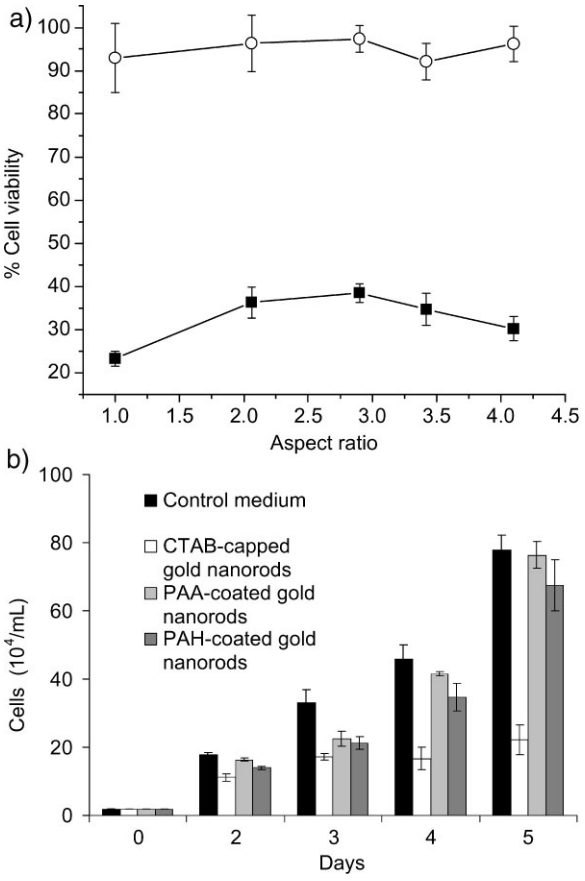

Figure 2. a) Viability of HT-29 cells exposed to 0.4 nM of either CTAB-capped gold nanorod solutions (■) or PAA-coated gold nanorod solutions (○) for four days as a function of gold nanorod aspect ratio. b) Growth of HT-29 cells exposed to 0.4 nM of CTAB-capped gold nanorod solutions for five days. Error bars represent one standard deviation.

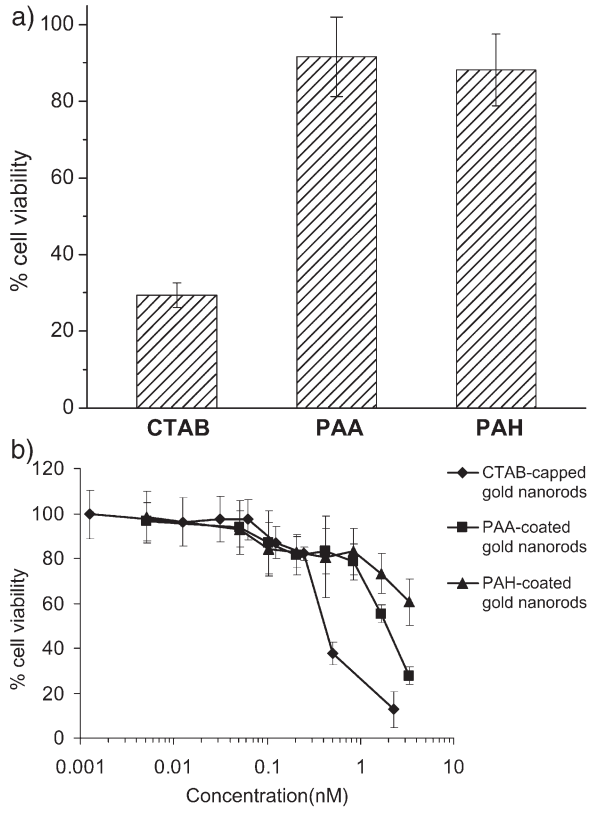

Figure 3. Viability of cells exposed to gold nanorods with different surface coatings. a) Viability of HT-29 cells exposed to 0.4 nM of CTAB-, PAA- and PAH-coated gold nanorod solutions for four days. Aspect ratios of all gold nanorods were 4.1. b) Dose-dependent viability of HT-29 cells exposed to increasing concentrations of CTAB-, PAA-, and PAH-coated gold nanorod solutions (aspect ratios of 4.1). Error bars represent one standard deviation.

representative aspect ratio of 4.1. Whereas the CTAB-capped gold nanorod solution was found to reduce cell viability to 30% at 0.4 nM nanorods, both PAA- and PAH-coated gold nanorod solutions were found to be relatively nontoxic (cell viability ~90%) at the same concentration. Measurements of cell growth (Figure 2b) agreed with the viability studies (Figure 3a). Dose-response studies (Figure 3b) showed that PAA- and PAH-coated nanorod solutions up to fivefold higher in concentration (>1 nM in particles) were nontoxic compared to the CTAB-containing solution. These results indicate that gold nanorods with either a positively or negatively charged polyelectrolyte layer are less toxic than the original CTAB-capped gold nanorod solution and thus cytotoxicity of nanoparticles are not correlated with its surface charge.

To test whether free CTAB arising from desorption or residual contamination was responsible for the cytotoxicity seen in the CTAB-capped nanorod solution, the nanoparticles were removed by centrifugation and the cytotoxicity of the resulting supernatants was compared with the original gold nanorod solutions. As the supernatants were colorless and the extinction coefficient of gold nanorods is $\sim 10^9\ M^{-1}\ cm^{-1}$, [23] this suggests that the gold nanorod concentration in the supernatants is subpicomolar in particles. The cytotoxicity of the colorless supernatant was found to be nearly identical to the cytotoxicity of its original deeply colored CTAB-capped gold nanorod solution (Figure 4). Liquid chromatography mass spectrometry was used to quantify the CTAB concentration in the supernatants, yielding values in the range of 0.2–0.3 μM. At these concentrations, the observed cell viability of the supernatants matched closely with the viability observed in the dose-response curve of CTAB alone (Figure S1, Supporting Information). CTAB concentrations in both PAA and PAH-coated gold nanorod supernatants were below the detection limit (about 4 pM). These results support the argument that the presence of free CTAB molecules is a more important factor in cellular cytotoxicity than nanoparticle surface charge, and that overcoating CTAB on the nanoparticles is an effective way to reduce their cytotoxicity.[11] In addition to desorbed or contaminating CTAB molecules, the supernatant solutions may also contain leftover metal ions that could contribute to the cytotoxicity. Inductively coupled plasma with atomic emission spectroscopy was employed to analyze the supernatants for their metal content. Gold and silver ion concentrations in the supernatants were below the detection limits of the instrument (~5 μM metal ions), a level we observed to be nontoxic for these ions (data not shown). These results further confirmed that gold nanorod solutions are not toxic by themselves, but

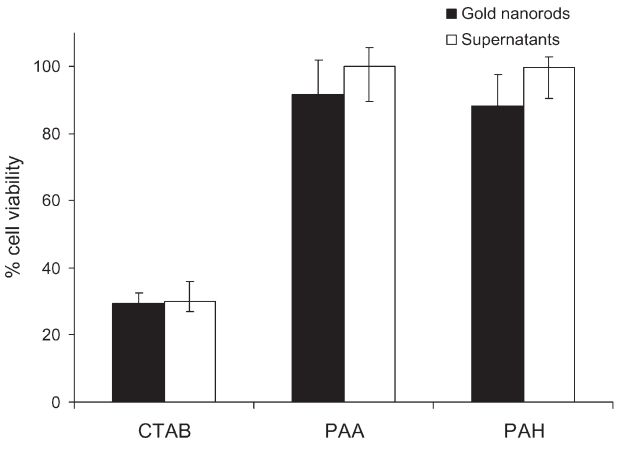

Figure 4. Viability of HT-29 cells exposed to 0.4 nM of CTAB-, PAA-, and PAH-coated gold nanorod solutions (filled bars) and their supernatants (open bars) for four days. Aspect ratios of all gold nanorods were 4.1. Error bars represent one standard deviation.

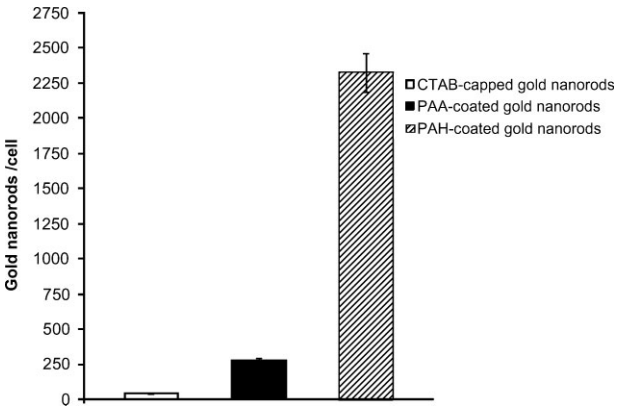

Figure 6. Cellular uptake of CTAB- (open bar), PAA- (filled bar), and PAH- (striped bar) coated gold nanorods as measured by ICP-MS. Gold nanorod solutions of aspect ratio 4.1 were added to the growth media to yield a final concentration of 3.3 pM (picomolar in gold nanorods). Cells were incubated for 24 hours before analysis (for details see Experimental Section). Error bars represent one standard deviation.

that free CTAB molecules are responsible for the cytotoxicity. These results are reminiscent of cytotoxicity studies of carbon nanotubes, in which byproducts of the manufacturing process are the toxic agents.[25] We had previously observed that CTAB-capped 18-nm nanospheres were not toxic in a different human cancer cell line, once excess CTAB was removed.[26] We re-examined CTAB-capped gold nanospheres in the HT-29 cells, and found that nanospheres of diameter 8.4 ± 1.5 nm and 18.0 ± 3.0 nm showed a minor reduction in viability (2% and 5%, respectively) at a nanoparticle concentration of 0.4 nM, whereas 24.0 ± 4.2-nm nanospheres reduced viability by 40% (Figure S2, Supporting Information). As was seen with the gold nanorod solutions, the supernatants from gold nanosphere solutions led to the same cell viability as the original nanosphere solutions (Figure S2, Supporting Information), suggesting that soluble components in the supernatant are responsible for the toxic effects.

Gold nanorods with the various surface coatings were taken up by the cells, as visualized by transmission electron microscopic (TEM) imaging of nanoparticles inside the cells (Figure 5). The uptake of gold nanorods inside the cells was also confirmed by using dark-field microscopy. Gold nanorods scatter light in the visible region of the spectrum due their strong longitudinal surface plasmon oscillation. Yellowish/greenish scattering is clearly visible for cells incubated with PAA and PAH coated nanorods compared to controls (cells alone; Figure S3, Supporting Information).

To quantify the number of gold nanorods that are taken up per cell, inductively coupled plasma mass spectrometry (ICP-MS) was used, which has a limit of detection of 60 parts per trillion for gold, or 0.20 fM for our gold nanorods of aspect ratio 4.1. In this experiment, the same numbers of cells were exposed to the same nontoxic concentration (0.2 nM) of CTAB, PAA, and PAH-coated gold nanorod solutions for 24 hours. Cell numbers for all the samples and controls were measured after 24 hours and the cell growth rate for the samples exposed to nanoparticles was found to be similar to the untreated controls. ICP-MS results indicated drastically different numbers of gold nanorods per cell: CTAB-capped gold nanorods, 45 ± 6 nanorods per cell; PAA-coated gold nanorods, 270 ± 20 nanorods per cell; PAH-coated gold nanorods, 2320 ± 140 nanorods per cell (Figure 6). ICP-MS data on the washings from the cells showed no detectable gold, suggesting that the nanorods per cell represent those nanorods that are either tightly bound to the cell membrane or actually internalized. Therefore, the surface coating of the nanorods apparently does influence the degree of cellular uptake.

The mechanism of cellular uptake for biomolecules in the size range of the nanorods has been suggested to be receptor-mediated endocytosis.[27] Cells have receptors that recognize proteins present in the serum-containing media. An investigation of the surface chemistry of the gold nanoparticles in the cellular media provided some interesting insights. After exposure to growth media containing

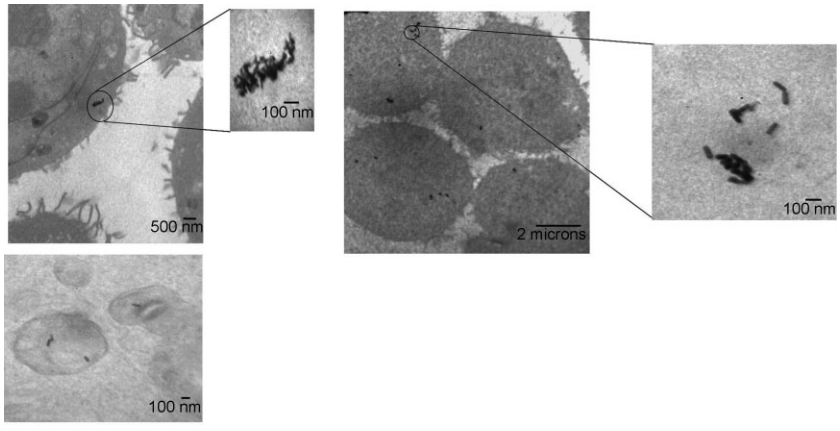

Figure 5. TEM images of left panels) CTAB-capped gold nanorods, right panels) PAA-capped gold nanorods inside HT-29 cells. All gold nanorods have an aspect ratio of 4.1.

NANO MICRO small

serum proteins followed by subsequent purification, the zeta potential for the originally positively charged gold nanorods (both CTAB and PAH coated) became negative (Figure 7). Moreover, all gold nanorods (CTAB, PAA, PAH) reached a similar zeta potential value of about −20 mV in 5 minutes after exposure to the media, which is the same zeta potential value of the growth media alone without nanorods. Other groups have observed that many nanomaterials adopt the same surface charge in biological media.[28] The main protein component in the media is bovine serum albumin, BSA, which has an isoelectric point of 4.6, and therefore at physiological pH has a negative effective surface charge (zeta potential = −20 mV).[29] These changes in nanorod zeta potential were not observed in the media lacking serum proteins (data not shown). The change in the zeta potential of the gold nanorods can be explained by the adsorption of BSA and other media proteins on the nanoparticle surfaces.[17] BSA adsorption on both positive and negative self-assembled monolayers on flat gold surfaces has been reported,[30] and the ability of this protein to adsorb to many surfaces is due to the presence of different domains with different charge density.[31] The adsorption of protein on the gold nanorods was confirmed by Fourier transform infrared (FTIR) measurements of amide I (~1650 cm^{-1}) and III (1300–1200 cm^{-1}) bands in the gold nanoparticles exposed to growth media, after purification by centrifugation (Figure S4, Supporting Information). UV/Vis absorbance spectra for gold nanorods exposed to growth media containing serum proteins have an additional peak at 275 nm, corresponding to the presence of aromatic protein residues. In addition, effective diameter of gold nanorods (CTAB, PAA, PAH) exposed to growth media containing serum albumin as measured by dynamic light scattering found to increase by 22–36% from the initial dimensions (Figure 8), consistent with protein adsorption.

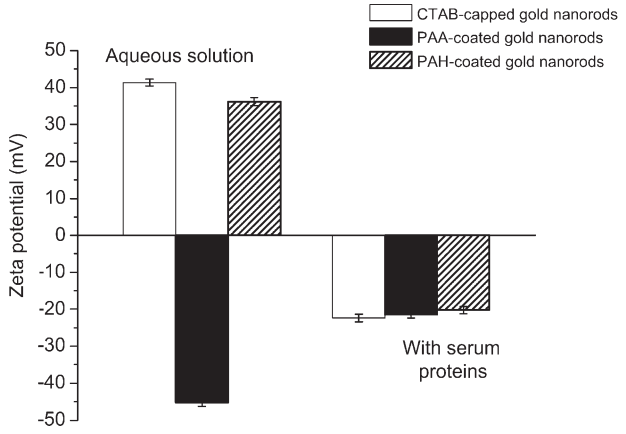

Figure 7. Effective surface charge (zeta potential) of gold nanorods coated with CTAB, PAA, and PAH in water before exposure to growth media and after exposure to growth media with serum proteins (containing 10% bovine serum albumin). All gold nanorods were centrifuged after 30 minutes of exposure and re-suspended in deionized water before measurements were obtained. Aspect ratio for all gold nanorods was 4.1. Error bars represent one standard deviation.

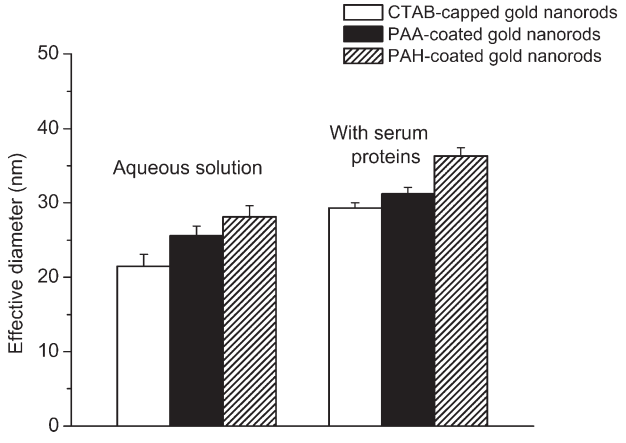

Figure 8. Effective hydrodynamic diameter measurements of gold nanorods coated with CTAB, PAA, and PAH in water before exposure to growth media and after exposure to growth media with serum proteins (containing 10% bovine serum albumin). All gold nanorods were centrifuged after 30 minutes of exposure and re-suspended in deionized water before measurements were obtained. Aspect ratio for all gold nanorods was 4.1. Error bars represent one standard deviation.

3. Discussion

The high promise of nanoparticles for biological applications is tempered by a lack of knowledge concerning the unintended consequences of the nanomaterials or the byproducts associated with their synthesis.[8] In this regard, the cytotoxicity of CTAB-capped gold nanorod solutions was found to be due to free CTAB and not necessarily the rods themselves, or residual metal ions. Polymer overcoating the CTAB-capped gold nanorods regardless of charge reduced the cytotoxicity, presumably by preventing desorption of CTAB molecules from the surface of the gold nanorods. However, we note that the concentration of free CTAB present in the gold nanorod solutions is in the range of 0.2–0.3 μM, which corresponds to 5–20% of the total CTAB bound to the nanorods. Therefore, CTAB bound to the nanorods is far less toxic than free CTAB. It is important to keep in mind that the number of particles per cell was kept constant when cells were exposed. Therefore, the particle surface area accessible to the cells varied, from smallest for 8-nm spheres to largest for nanorods with an aspect ratio of 4.1. Taken together, the results with nanorods and nanospheres suggest that CTAB desorption from gold nanoparticles likely reaches a threshold level based on nanoparticle size and surface area; at the constant dose experiments we performed, the 8-nm spheres and 18-nm spheres had the least surface area and therefore the least potential CTAB desorption. More thorough studies of CTAB desorption kinetics as a function of particle size and shape are in progress.

Serum proteins from the growth media were found to adsorb on gold nanoparticles, which slightly increased the net size of the nanoparticles and also converted the surface charge to that of BSA. The results provide direct evidence that, regardless of the original surface charge, gold nanorods can adsorb serum proteins, thus adopting the physiochemical characteristics of biological macromolecules. Adsorbed BSA (or other serum proteins) may facilitate the uptake of

nanomaterials via receptor-mediated endocytosis.[32,33] Our results show that each of the gold nanorod preparations, regardless of initial surface charge, adopted the charge of serum proteins and were found to enter the cells. The extent of uptake, rigorously quantified by ICP-MS, was PAH $\gg$ PAA > CTAB, which does not support the notion that initial surface charge is a simple predictor of nanoparticle uptake and cytotoxicity.[11–16] Indeed, nanoparticle uptake into cells is likely governed by the type of adsorbed proteins and their relative orientations on the nanoscale curved surfaces; by presenting different chemical ''faces'' to the cells, different receptor-mediated endocytosis pathways may be exploited for cell entry.[32–34] BSA alone has at least four known cell surface receptors that can independently bind and endocytose it into cells.[34] However, it is also known that protein adsorption to surfaces may change over time, with higher-binding-constant proteins replacing initial weak adsorbers.[35] Clearly, studies of nanoparticles surfaces as a function of time after exposure to serum or other complex mixtures are needed to fully understand the mechanism, fate, and transport of nanomaterials in a natural environment.[19]

4. Conclusions

In conclusion, our results suggest that predicting and examining the biological properties of nanomaterials should include studies to examine nanomaterials after exposure to biological systems. Future toxicological studies of all classes of nanoparticles should focus on rates of desorption of crucial (toxic) nanoparticle constituents in order to determine negative consequences of extended exposure. The utilization of nanoparticles for biomedical applications should take into account or even exploit nanoparticle-protein interactions.

5. Experimental Section

Materials: Chloroauric acid ($HAuCl_4.3H_2O$, 99.9%), sodium borohydride ($NaBH_4$, 99%), silver nitrate ($AgNO_3$, 99+%), ascorbic acid (99+%), poly(alliamine hydrochloride), (PAH, MW ~15000 g/mole) and poly(acrylic acid, sodium salt) (PAA, MW ~15000 g/mole) were obtained from Aldrich and used as received. Cetylltrimethylammonium bromide (CTAB, 99%, Sigma Ultra) was obtained from Sigma Chemicals and used as received. All solutions were prepared with Barnsted E-PureTM 18 MΩ water. Glassware was cleaned with aqua regia and rinsed thoroughly with Barnsted E-PureTM water. Human adenocarcinoma HT-29 cells (ATCC, Manassas, VA) were maintained in Dulbecco's Modified Eagle Medium – DMEM (GIBCO, Invitrogen, Carlsbad, CA) supplemented with 10% fetal bovine serum (FBS) (Hyclone, Logan, UT) and 1% penicillin/streptomycin (Hyclone) at 37 °C and 5% CO_2 (Fisher Scientific). MTT (thiazolyl blue tetrazolium bromide) dye was purchased from Sigma.

Standard solutions (1000 μg mL^{-1}) of gold and iridium were purchased from High Purity Standards (Charleston, SC). Optima grade HCl, HNO_3 were purchased from Thermo Fischer Scientific (Suwanee, GA).

CTAB capped gold nanorod synthesis: Gold nanorods were synthesized as previously described.[20] A solution 2.5×10^{-4} M $HAuCl_4$ was prepared in 0.1 M CTAB. $NaBH_4$ (600 μL, 10 mM) at 0 °C was added to the gold/CTAB solution (10 mL) with vigorous stirring for 10 min. The resulting seed nanoparticles were used in the synthesis of gold nanorods. Briefly, the following aqueous solutions were added to a 125 mL conical flask, in the following order: CTAB solution (95 mL, 0.1 M), silver nitrate solution (0.1–1 mL, 10 mM; aspect ratio of the gold nanorod is controlled by varying silver nitrate concentration), chloroauric acid (5 mL, 10 mM). To this solution ascorbic acid (0.55 mL, 0.1 M) was added with gentle mixing. Finally seed solution (0.12 mL) was added and the entire solution was mixed and left undisturbed overnight (14–16 hours). The colored gold nanorod solution was purified by centrifugation to remove excess CTAB (twice at 14000 rpm, 3 min each). Attempts to remove CTAB by dialysis led to irreversible nanoparticle aggregation, unsuitable for the present work.

PAA-coating of gold nanorods:[21] To purified CTAB-capped gold nanorod solution (1 mL), PAA solution (200 μL, 10 mg/mL prepared in 10 mM NaCl solution) and NaCl solution (100 μL, 10 mM) were added simultaneously. The resulting solution was mixed gently for 30 minutes to allow for complete polymer coating. To get rid of the excess PAA polymer after coating, the coated gold nanorod solution was centrifuged for 3 min at 14 000 rpm. The pellet was re-suspended in DI water for further study.

PAH-coating of gold nanorods:[21] To the purified PAA-coated gold nanorod solution (1 mL), PAH solution (200 μL, 10 mg/mL prepared in 10 mM NaCl solution) and NaCl solution (100 μL, 10 mM) were added simultaneously. The resulting solution was mixed gently for 30 min to allow for complete polymer coating. To get rid of the excess PAH polymer after coating, the coated gold nanorod solution was centrifuged for 3 min at 14000 rpm. The pellet was re-suspended in DI water for further study.

Characterization: Absorption spectra were taken on a CARY 500 Scan UV/Vis NIR spectrophotometer. Absorbance values for the MTT assay were collected on ELX808 Ultra microplate reader (Bio-tek, Winooski, VT). Transmission electron microscopy (TEM) data for gold nanoparticles were obtained with a Hitachi H-8000 electron microscope operating at 200 kV. TEM grids were prepared by drop-casting the purified gold nanorod solution (7 μL) on the TEM grids and drying them in atmosphere. FTIR spectra of drop-dried samples were collected in reflectance mode with a Nexus Thermo-Nicolet 470 series FTIR instrument coupled with a Thermo-Nicolet continuum FTIR microscope. The samples were prepared by placing a few drops of the gold nanorods solution on Si (111) wafers and drying in a covered Petri dish. FTIR spectra were recorded over 128 scans of each sample with a resolution of 4 cm^{-1} and the background spectra were automatically subtracted. Gold and silver ion concentrations in the supernatants were determined using Varian vista inductively coupled plasma atomic emission spectrometer (ICP-AES). All ICP-AES runs were carried out in triplicate. Zeta-potential and dynamic light scattering measurements were performed on a Brookhaven Zeta PALS instrument. A microcentrifuge (Eppendorf model 5418, Fisher-Thermo Electron) was used in gold nanorod synthesis and purification as detailed below. Bright-field microscope images

NANO MICRO small

were taken using Axiovert 40 Inverted transmitted-light microscope (Zeiss, Gottingen, Germany). Dark field images were obtained using Nikon Eclipse Model ME600L microscope.

Cell viability and growth determination: Cell viability was measured using the MTT assay and cell growth was determined by cell counting following four days of continuous exposure to the gold nanoparticles. For viability, exponentially growing cells were dispensed into a 96-well flat bottom plate at a concentration of 10^3 cells/well (100 μL). After allowing 24 hours for cell attachment, gold nanoparticle solutions (i.e., gold nanorods, gold nanospheres) were diluted appropriately in fresh media and added (100 μL), 6 wells per sample. The media was not changed during the incubation. Following four days of incubation, cell viability was determined by the addition of MTT (20 μL, 5 mg/mL dye in sterile PBS). The plate was incubated for an additional 5 hours at 37 °C and 5% CO_2, allowing viable cells to convert the pale yellow MTT to an insoluble purple dye. The insoluble dye was collected by centrifugation at 300 g for 5 min. The media was carefully removed and the collected dye was dissolved in dimethyl sulfoxide (200 μL). Absorbance values at 595 nm were collected and cell viability was calculated as a percentage compared to untreated control cells. For cell growth experiments, exponentially growing HT-29 cells were seeded at a concentration of 2×10^4 cells/ml in 24-well dishes with 1 mL of growth media per well. The dishes were incubated at 37 °C and 5% CO_2 (Day 0). After 24 hours (day 1), CTAB-capped, PAA-coated and PAH coated gold nanorods were added in wells to achieve a final concentration of 0.4 nM. Growth media lacking gold nanorods was used as control. Cell growth rates were measured at days 2, 3, 4, and 5. The data shown is an average of three experiments.

Cellular uptake of gold nanoparticles quantitation by ICP-MS: An Element 1 high-resolution inductively coupled plasma mass spectrometry (ICP-MS) instrument (Thermo Finnigan, Bremen, Germany) was used for gold detection. Aqueous samples were introduced using the high-efficiency HF Apex introduction system (Elemental Scientific, Omaha, NE). Samples were introduced at a rate of 100 μL min^{-1} with a PFA microflow nebulizer (Elemental Scientific, Omaha, NE). Gas-flow rates and RF power was adjusted daily to optimize the intensity and stability of gold ions, m/z 197, and iridium, m/z 193, while minimizing the oxide formation, which was typically under 0.2% (UO/U). Instrument drift was corrected by locking onto the Iridium (Ir^{193}) peak as well as running gold standards through the sample sequences. All samples were run in triplicate. Standard addition was used for gold quantitation. Raw data from the mass spectrometer was exported to MS Excel spreadsheet for analysis. The standard deviation of triplicate peak areas were used to calculate error of the standard addition, and uncertainties were propagated by standard methods. All samples and standards were prepared in a class 1000 cleanroom. Working standards were prepared daily by gravimetric determination and serial dilution from the standard solutions. All vials, sample containers, and consumables were placed in aqua regia for 3 hours, and then boiled in DW over night to remove any Cl_2 (g) and NO (g) that may of diffuse into the Teflon. Then the vials, sample containers, and consumables were washed with 2 M HCl for 72 hours, triply rinsed with 18 MΩ water, and allowed to dry in a class 1000 cleanroom before use.

Gold nanomaterial loss by container surface complexation/sorption was examined by spiking a known concentration of gold nanorods into the growth medium placed in 60-mm cell-culture dish without cells. The growth media was mixed gently using a pipette and an aliquot from the growth media (10 μL) was immediately withdrawn and analyzed. The dishes were incubated for 24 hours. After 24 hours, an aliquot from the growth media (10 μL) was withdrawn and analyzed. The ratio between the initial concentration and the concentration after 24 hours was calculated for CTAB, PAA, and PAH coated gold nanorods.

To quantify the gold nanorod associated with the cells, gold nanorod solution of aspect ratio 4.1 were added to the growth media to yield a final concentration of 3.3×10^{-12} M (gold nanorods) for all CTAB, PAA, and PAH coatings. Cells were incubated for 24 hours and then the growth media was removed and washed three times with PBS buffer solution. Cells were washed three times with PBS buffer, trypsinized and counted. Cells (1.2×10^6) from each incubation (in triplicates) were collected in separate centrifuge tubes, washed three times via centrifugation at 1200 rpm for 5 min each. The supernatant of the last wash was analyzed for gold. Cell pellets were spiked with an Ir^{193} internal standard and digested with optima aqua regia (400 μL, Optima acids) for 24 hours in a 2 mL Teflon bomb at 150 °C. After digestion samples were analyzed by ICP-MS.

Mass spectrometry: ESI-LC-MS was carried out in the positive-ion mode on a Waters Micromass QuattroLC triple quadrupole mass spectrometer equipped with an Agilent 1100 Binary HPLC system and an ES Industries Chromegabond WR C-8 column (5-μm particles; 15 cm × 2.0 mm). The solvent system consisted of a binary linear gradient using water (A) and acetonitrile (B) both containing 0.1% formic acid, at a flow rate of 200 μL/min. The gradient began at 60%B progressing to 90%B over 30 min. Benzyldimethyltetradecyl ammonium chloride was used as internal standard. The electrospray needle voltage was held at 3000 V and the sample cone at 25 V. Selected ion recording of the cations for the cetyltrimethylammonnium bromide (CTAB) analyte and the internal standard was at $m/z = 284.3$ and 332.3 respectively. The internal standard method was used to construct the calibration curve using four points ranging from 2 ppb to 400 ppb CTAB with each standard and sample containing 130 ppb internal standard. All standards were measured in triplicate. All samples were diluted in 100% methanol and placed in 2 mL glass autosampler vials prior to analysis.

Determination of interaction of gold nanoparticles with growth media: Purified gold nanoparticles (0.4 nM, concentration in particles) were mixed 1:1 volume ratio with DMEM media (containing 10% fetal bovine serum). The UV/Vis spectrum for the mixture was obtained as a function of time. After 30 min, the mixture was centrifuged for 3 min at 14 000 rpm and the resulted pellet was re-suspended in DI water. The resulting solution was analyzed by obtaining zeta potential and dynamic light scattering measurements and UV/Vis and FTIR spectra.

Preparation of cell samples for transmission electron microscopy: HT-29 cells growing in the log phase were plated at a density of 5×10^4 cells/mL in a 100 mm dish. After allowing 24 hours for cell attachment, the gold nanorod solution was added to the dishes. Following another 24 hours of incubation of the gold

nanorods with the cells, cells were trypsinized and washed three times with sterile phosphate buffered saline (PBS) before being collected by centrifuging at 2000 rpm for 10 min. The cells were fixed in cacodylate buffered (pH 7.2) 2.5% glutaraldehyde for 2–3 hours at room temperature and washed three times in 0.1 M cacodylate buffer at 10 min interval. The samples were then post-fixed in cacodylate buffered 1% osmium tetroxide for 1–1.5 hours at 4 °C and washed 3 times in cacodylate buffer (0.1 M). Later, the samples were dehydrated in a series of ethanol washes (50%, 70%, 80%, 95%) for 10 min each. Additionally, samples were dehydrated twice in 100% ethanol (10 min each) and embedded in Spurrs resin. Ultrathin sections were cut using a Diatome diamond knife and were stained with uranyl acetate followed by lead citrate.

Acknowledgements

The authors thank Dr. W. E. Cothman for LC-MS data acquisition and Dr. S. Ghoshroy for assistance with the TEM. The National Science Foundation (CHE-0701406), the University of South Carolina NanoCenter, and the University of South Carolina's Office of the Vice President for Research and Health Sciences are acknowledged for funding.

[1] G. Han, P. Ghosh, V. M. Rotello, *Nanomed.* **2007**, *2*, 113–123.
[2] A. K. Salem, P. C. Searson, K. W. Leong, *Nat. Mater.* **2003**, *2*, 668–671.
[3] C. J. Murphy, A. M. Gole, S. E. Hunyadi, J. W. Stone, P. N. Sisco, A. M. Alkilany, B. E. Kinard, P. Hankins, *Chem. Commun.* **2008**, 544–557.
[4] J. W. Stone, P. N. Sisco, E. C. Goldsmith, S. C. Baxter, C. J. Murphy, *Nano Lett.* **2007**, *7*, 116–119.
[5] H. Wang, T. B. Huff, D. A. Zweifel, W. He, P. S. Low, J. X. Cheng, *Proc. Natl. Acad. Sci. USA* **2005**, *102*, 15752–15756.
[6] I. H. El-Sayed, X. Huang, M. A. El-Sayed, *Nano Lett.* **2005**, *5*, 829–834.
[7] X. Huang, P. K. Jain, I. H. El-Sayed, M. A. El-Sayed, *Nanomed.* **2007**, *2*, 681–693.
[8] a) M. N. Helmus, *Nature Nanotech* **2007**, *2*, 333–334; b) V. L. Colvin, *Nature Biotechnol.* **2003**, *21*, 1166–1170; c) A. Nel, T. Xia, L. Madler, N. Li, *Science* **2006**, *311*, 622–627; d) K. A. D. Guzman, M. R. Taylor, J. F. Banfield, *Environ. Sci. Technol.* **2006**, *40*, 1401–1407; e) G. Obedrdoster, E. Obedrdoster, J. Environ, *Health prespect.* **2005**, *113*, 823–839; f) R. Own, R. Handy, *Environ. Sci. Technol.* **2007**, *41*, 5582–5588; g) A. D. Maynard, R. J. Aitken, T. Butz, V. Colvin, K. Donaldson, G. Oberdoster, M. A. Philbert, J. Ryan, A. Seaton, V. Stone, S. S. Tinkle, L. Tran, N. J. Walker, D. B. Warheit, *Nature* **2006**, *444*, 267–269.
[9] N. Lewinski, V. Colvin, R. Drezek, *Small* **2008**, *4*, 26–49.
[10] P. Nativo, I. A. Prior, M. Brust, *ACS Nano* **2008**, *2*, 1639–1644.
[11] T. S. Hauck, A. A. Ghazani, W. C. Chan, *Small* **2008**, *4*, 153–159.
[12] C. M. Goodman, C. D. McCusker, T. Yilmaz, V. M. Rotello, *Bioconjug. Chem.* **2004**, *15*, 897–900.
[13] S. Hong, A. U. Bielinska, A. Mecke, B. Kelzler, J. L. Beals, X. Shi, L. Balogh, B. G. Orr, J. R. Baker, M. M. Banaszak Holl, *Bioconjugate Chem.* **2004**, *15*, 774–782.
[14] A. Nan, X. Bai, S. J. Son, S. B. Lee, H. Ghandehari, *Nano Lett.* **2008**, *8*, 2150–2154.
[15] I. Slowing, B. G. Trewyn, V. S.-Y. Lin, *J. Am. Chem. Soc.* **2006**, *128*, 14792–14793.
[16] F. Hoffmann, J. Clinatl Jr, H. Kabičková, J. Cinatl, J. Kreuter, F. Stieneker, *Int. J. Pharm.* **1997**, *157*, 189–198.
[17] I. Lynch, T. Cedervall, M. Lundqvist, C. Cabaleiro-Lago, S. Linse, K. A. Dawson, *Adv. Colloid Interface Sci.* **2007**, *134–135*, 167–174.
[18] I. Lynch, *Physica A* **2007**, *373*, 511–520.
[19] T. Cedervall, I. Lynch, M. Foy, T. Berggard, S. C. Donnelly, G. Cagney, S. Linse, K. A. Dawson, *Angew. Chem. Int. Ed.* **2007**, *46*, 5754–5756.
[20] T. K. Sau, C. J. Murphy, *Langmuir* **2004**, *20*, 6414–6420.
[21] A. M. Gole, C. J. Murphy, *Chem. Mater.* **2005**, *17*, 1325–1330.
[22] T. K. Sau, C. J. Murphy, *Langmuir* **2005**, *21*, 2923–2929.
[23] C. J. Orendorff, C. J. Murphy, *J. Phys. Chem. B* **2006**, *110*, 3990–3994.
[24] T. Mosmann, *J. Immunol. Methods* **1983**, *65*, 55–63.
[25] K. Pulskamp, S. Diabate, H. F. Krug, *Toxicol. Lett.* **2007**, *168*, 58–74.
[26] E. E. Connor, J. Mwamuka, A. Gole, C. J. Murphy, M. D. Wyatt, *Small* **2005**, *1*, 325–327.
[27] M. A. Dobrovolskaia, D. E. McNeil, *Nature Nanotech.* **2007**, *2*, 469–478.
[28] T. Xia, M. Kovochich, J. Brant, M. Hotze, J. Sempf, T. Oberley, C. Sioutas, J. I. Yeh, M. R. Wiesner, A. E. Nel, *Nano Lett.* **2006**, *6*, 1794–1807.
[29] T. Peters, Jr, *All About Albumin: Biochemistry, Genetics, and Medical Applications*, Academic Press, San Diego, USA 1996, p. 25.
[30] V. Silin, H. Weetall, D. J. Vanderah, *J. Colloid Interface Sci.* **1997**, *185*, 94–103.
[31] K. Rezwan, L. P. Meier, M. Rezwan, J. Voros, M. Textor, L. J. Gauckler, *Langmuir* **2004**, *20*, 10055–10061.
[32] S. D. Conner, S. L. Schmid, *Nature* **2003**, *422*, 37–44.
[33] K. J. Kim, A. B. Malik, *Am. J. Physiol Lung Cell Mol. Physiol.* **2003**, *284*, L247–L259.
[34] J. E. Schnitzer, P. Oh, *J. Biol. Chem.* **1994**, *269*, 6072–6082.
[35] L. Vroman, A. L. Adams, *Surf. Sci.* **1969**, *16*, 438–446.

Received: October 17, 2008
Revised: December 29, 2008
Published online: February 18, 2009

